How does the geometry affect the criticality in two-component spreading phenomena?

1998 J. Phys. A: Math. Gen. 31 9199

(http://iopscience.iop.org/0305-4470/31/46/010)

J. Phys. A: Math. Gen. **31** (1998) 9199–9208. Printed in the UK PII: S0305-4470(98)95570-6

How does the geometry affect the criticality in two-component spreading phenomena?

N I Lebovka†‡§ and N V Vygornitskii†

† Institute of Biocolloid Chemistry NASU, 2 bulv. Vernadskogo, Kyiv 252142, Ukraine
‡ Kyiv Mogyla Academy University, 2 vul. Scovorody, Kyiv 252145, Ukraine

Received 1 July 1998

Abstract. We study numerically the two-component spreading model (SMK) for concave and convex radial growth two-dimensional geometries. The seed is chosen to be an occupied circle line, and the growth spreads inside the circle (concave geometry) or outside the circle (convex geometry). On the basis of a generalized diffusion–annihilation equation for domain evolution, we derive mean-field relations that describe quite well the results of numerical investigations. We conclude that the intrinsic universality of the SMK does not depend on the geometry, and that the dependence of criticality on curvature observed in numerical experiments is only an apparent effect. We discuss the dependence of the apparent critical exponent χ_a upon the growth geometry and initial conditions.

1. Introduction

Nonequilibrium growth and spreading phenomena are common in nature. Examples include such processes as irreversible adsorption or deposition on the surface, liquid invasion in porous media, forest fire, crystal growth, evolution of damage in mechanical or electrical systems, epidemic spreading, etc. Presently, different varieties of such phenomena are extensively studied using numerical models [1–6]. The simplest models deal with ideal species of the same size (or type) and the main focus of attention is investigation of the interrelations between growth mechanism, surface equilibration efficiency, details of interparticle interactions and pattern morphology.

But ideal systems of monospecies rarely occur in nature and certain variations of physical or structural properties are almost always present in such systems. The nonideal polydisperse or multicomponent systems are of great scientific and practical interest [7, 8]. Recently, various growth models with two species or phases in competition [9–14], and also the multicomponent Potts growth model [15, 16] have been investigated. The two-component growth model of Saito and Muller-Krumbhaar (SMK) [9] generalizes the Eden model [17] for the case of two different species (A and B) competition. The authors [9] observe the criticality of the two-dimensional model for the case of equal growth rates of two components in a half-space planar geometry, i.e. for the case where the growth starts from a linear seed line. This criticality results from the rules of species attachment at the growing front, which exclude the nucleation of A species in the neighbourhood of a domain consisting only of B species, and vice versa. The model reveals the competitive growth of separate

§ Author to whom correspondence should be addressed. E-mail address: lebovka@roller.ukma.kiev.ua

0305-4470/98/469199+10$19.50

domains and their coarsening. In the limit of large-time or, equivalently, of a large front height (h), power-law decay is found for the number of interdomain boundaries N_{AB},

$$N_{AB} \sim h^{-\chi} \tag{1}$$

where $\chi = \frac{2}{3}$ is the critical exponent for meandering interfaces [18]. More recently, Vandewalle and Ausloos [10] have concluded that the criticality of the SMK model is not universal and depends on the assumed geometry of the two-component propagation. They have shown that if the growth starts from a central site of the initial AB configuration, the value of the critical exponent χ may differ considerably from that observed for the half-space planar geometry ($\chi = \frac{2}{3}$). It should be noted that the geometry can affect the fractal dimension of a diffusion limited aggregation-like pattern in a closed cavity, as was observed in [19]. Recently, Batchelor *et al* [20] have shown that, for the usual two-dimensional radial Eden model, the growing scaling exponent β governing the interface roughening considerably exceeds the value of $\beta = \frac{1}{3}$, which is typical for stochastic growth on a planar substrate (in $1+1$ dimensions), and only approaches this value in the asymptotic limit of the very large Eden cluster radius.

This paper studies the kinetics of two-component spreading on curved surfaces in an assumed SMK model. The evolution of domains, their diffusion and annihilation, takes place on a two-dimensional square lattice, and the growth spreading is either confined inside the circle (concave geometry), or takes place outside the circle (convex geometry). For infinitely large radius of the circle, $R \to \infty$, we revive half-space or planar geometry [9]; for the other limit of $R \to 0$ we consider the spreading in a free space [10]. This modified model allows us more precisely to control the influence of geometry on criticality. We use the mean-field diffusion–annihilation approach and SMK model simulations for the calculation of density profiles for the wall boundaries between A and B domains as a function of distance from the seed wall h for seed circles of different radius, R. It will be shown that even in the case where criticality remains unchanged, the apparent value of the critical exponent of domain wall spatial distribution may vary, and that it depends on the geometry and initial distribution of A and B domains on the seed line.

The remainder of the paper is organized as follows. Section 2 presents a brief description of the model and simulation details. Section 3 is devoted to our results and discussion. Section 3.1 contains theoretical discussion on the issue of universality for the competitive growth model with curved seed line. Here, we use the mean-field approach to describe the domain wall coalescence. In section 3.2 we present the results of a numerical simulation, performed using the SMK algorithm of [9], in order to test the theory exploited in section 3.1. Section 4 contains our conclusions.

2. Model and simulation details

We have used the simple two-component SMK growth model [9] with equal growth rates for the two components. The simulation takes place on a square lattice. In this model, as in the Eden model, new particles attach to the growing cluster only along its perimeter. However in the SMK model the probability of filling any empty perimeter site either by A or by B species is in proportion to their concentration on the surface at the propagation front. Growth starts from a circular seed line and develops as growth front propagation for two different cases.

- Inside circular closed cavity. This is the case of concave geometry, or inside propagation (IP).

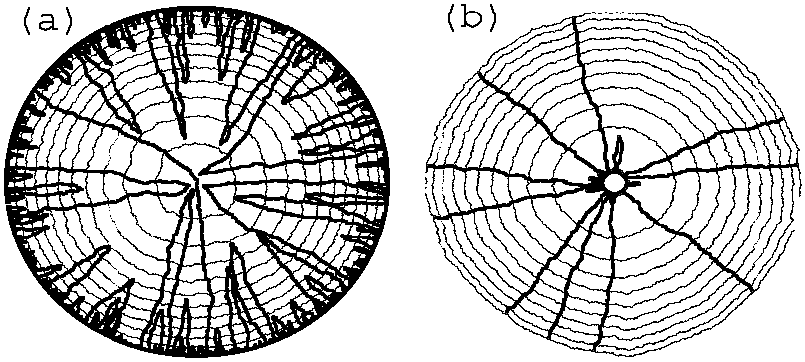

Figure 1. The typical growth spreading (*a*) inside the circular cavity of radius $R = 1000$ and (*b*) outside the circular exclusion of radius $R = 60$ for the two-species SMK model. The light concentric circles are the time snapshots of fronts for each next group of 300 000 particles attachment. The heavy lines show the AB domain interfaces.

• Outside the circular closed cavity. This is the case of convex geometry, or outside propagation (OP).

The maximal size of studied systems was 2000×2000 grid points and the intergrid distance was set as $d = 1$. For each case, 100–500 samples were averaged.

The simulation was carried out for differently ordered initial configurations, including the case of the maximal density of domain boundaries with short correlation length $\lambda_d = 1$, where single A and B alternate, as:

...	A	B	A	B	A	B	A	B	A	B	A	B	...

(2)

Lower densities of domain boundaries, with larger correlation length ($\lambda_d = 3$ for the case displayed), when there is an alternation of larger A and B domains with equal λ_d length were also considered, as:

...	A	A	A	B	B	B	A	A	A	B	B	B	...

(3)

If the initial number of domain boundaries is equal to N^0_{AB}, then the initial linear density of the domain walls will be equal to $\rho_0 = N^0_{AB}/L$, where $L = 2\pi R$ is the length of the seed line. For the case displayed as the seed line (2) we have $\rho_0 = \rho_{\max} \approx 1$ and

$$N^0_{AB} = N_{\max} \approx 2\pi R \tag{4}$$

and for the more common case displayed as the seed line (3) we have $\rho_0 \approx 1/\lambda_d$ and $N^0_{AB} \approx 2\pi R/\lambda_d$.

Figure 1 shows the typical spreading patterns of (*a*) the IP case with the radius of the closed cavity $R = 1000$ and (*b*) of the OP case with radius of circular exclusion $R = 60$. The light concentric circles are time snapshots of the front evolution at the moment of each next 300 000 particles attachment. The heavy lines show the AB interdomain boundaries. In the OP case the simulation terminates when the maximal radius of growth front $r_{\max}$ reaches the boundaries of system ($r_{\max} = 1000$). The initial density of boundaries is chosen to be maximal, $\rho_0 = \rho_{\max} \approx 1$, as displayed in the seed line (2). Note, that for both IP and OP cases we observe a generally quick decrease of the number of interdomain boundaries N_{AB} in initial periods of time, near to the surface of circular seed line.

3. Results and discussion

3.1. Mean-field approach

The domain evolution can be described in terms of an annihilation reaction of domain boundaries. If we associate each domain boundary with a phantom particle $\hat{A}$, then we can consider domain coarsening as a diffusion–annihilation reaction of a $\hat{A} + \hat{A} \rightarrow \emptyset$ [9] type. For a linear seed line, the time evolution of the density, $\rho = N_{AB}/L$, satisfies a mean-field rate equation

$$\frac{\mathrm{d}\rho}{\mathrm{d}h} = -a\rho^{1+1/\chi} \tag{5}$$

giving $\rho \sim h^{-\chi}$, where h is the height of the front, which is equivalent to the time, and a is the annihilation rate constant.

We have $\chi = \frac{1}{2}$ for normal Brownian motion [21–23], and $\chi = \frac{2}{3}$ for a two-species Eden [18] or SMK [9] model.

Using the simulation for planar geometry, we have estimated the annihilation rate constant as

$$a = 2.5 \pm 0.2 \tag{6}$$

where the data used in estimation were averaged over 100 different samples.

In the case of radial geometry, equation (5) should be modified. Here we have an additional source of ρ rate variations due to the spreading front shrinkage, or dilation, for the cases of growth spreading inside the circle (concave geometry), or outside it (convex geometry), respectively. The domain density ρ at the distance of $r = R \mp h$ from the centre of the seed circle is equal to

$$\rho = \frac{N_{AB}}{2\pi(R \mp h)} \tag{7}$$

where h is the distance from the seed circle, and, here and hereinafter, the upper sign $(-)$ corresponds to the front spreading inside the seed circle (IP case, concave geometry) and the under sign $(+)$ corresponds to the front spreading outside the seed circle (OP case, convex geometry). Taking (7) into account, we obtain (instead of (5)) the following rate equation for the above-mentioned cases of radial spreading with $\rho(0) = \rho_0$ as the initial condition:

$$\frac{\mathrm{d}\rho}{\mathrm{d}h} = -a\rho^{1+1/\chi} - \frac{\rho}{R \mp h}. \tag{8}$$

Introducing the new scaled variables $y = \rho R^{\chi}$, and $x = h/R$, we can rewrite (8) in a scaled form

$$\frac{\mathrm{d}y}{\mathrm{d}x} = -ay^{1+1/\chi} - \frac{y}{1 \mp x}. \tag{9}$$

Equation (9) is a Bernoulli equation and with substitution of $t = y^{-1/\chi}$ it reduces to

$$\frac{\mathrm{d}t}{\mathrm{d}x} - \frac{t}{1 \mp x} = \frac{a}{\chi}. \tag{10}$$

The solution of (10) with the initial condition of $t(0) = t_0 = \rho_0^{-1/\chi}/R$ has the following form

$$t(x) = t_0(1 \mp x)^{1/\chi}[\pm V(1 \mp x)^{1-1/\chi} + 1 \mp V] \tag{11}$$

where

$$V = a/(t_0(1-\chi)) = aR\rho_0^{1/\chi}/(1-\chi). \tag{12}$$

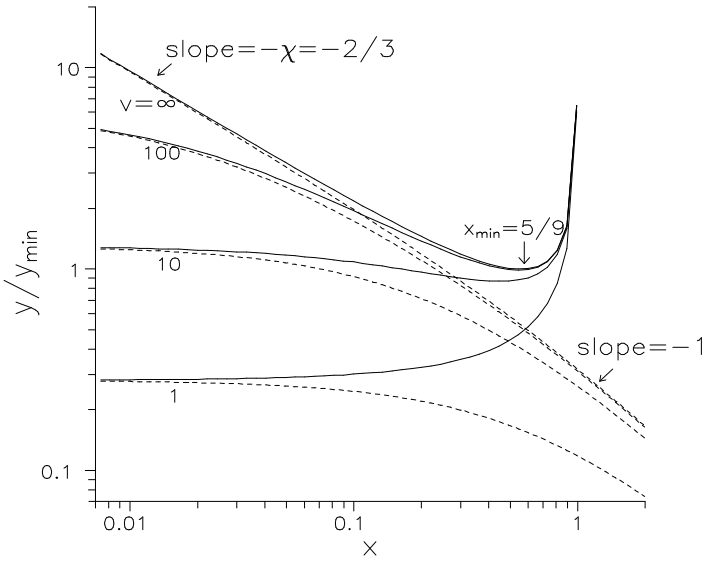

Figure 2. The mean-field dependence of the scaled density $y/y_{\min}$ ($y = \rho R^{\chi}$) versus scaled height of the front $x = h/R$ for the growth spreading inside the circular cavity (full curves) and outside the circular exclusion (broken curves) at different values of $V = aR\rho_0^{1/\chi}/(1-\chi)$. The value of $y_{\min}$ as defined by (16) corresponds to the minimum of $y(x)$ function in the point $x = x_{\min} = \frac{5}{9}$ (for $\chi = \frac{2}{3}$, see (15)) for growth spreading inside the circular cavity in the limit of $V \to \infty$.

Taking into account the inverse substitution $y = t^{-\chi}$, we obtain the following final solution of differential equation (9)

$$y(x) = \frac{y_0}{(1 \mp x)[\pm V(1 \mp x)^{1-1/\chi} + 1 \mp V]^{\chi}} \tag{13}$$

where $y_0 = \rho_0 R^{\chi}$.

For the IP case, when the spreading takes place inside the circle, the value $y(x)$ goes through the minimum at the point of

$$x_{\min}(V) = \begin{cases} 1 - \left(\dfrac{\chi}{1 - 1/V}\right)^{\frac{\chi}{\chi-1}} & \text{for } V \geqslant 1/(1-\chi) \\ 0 & \text{for } V < 1/(1-\chi). \end{cases} \tag{14}$$

For the case when $V \to \infty$, we have

$$x_{\min} = \lim_{V\to\infty} x_{\min}(V) = 1 - \chi^{\frac{\chi}{\chi-1}} \tag{15}$$

and

$$y_{\min} = \lim_{V\to\infty} y(x_{\min}) = a^{-\chi}\chi^{\frac{-\chi^2}{1-\chi}}. \tag{16}$$

Figure 2 presents the $y/y_{\min}$ versus x dependencies obtained from (13) and (16) for $\chi = \frac{2}{3}$ at different values of V for the cases of growth spreading inside the circle (full curves) and outside the circle (broken curves). The slope value $-\frac{2}{3}$ accounts for the slope of lines in the limit of $V \to \infty$ for the spreadings both inside and outside the circle, and the slope value -1 accounts for the line slopes in the limit of $x \to \infty$ for the growth spreading outside the circle.

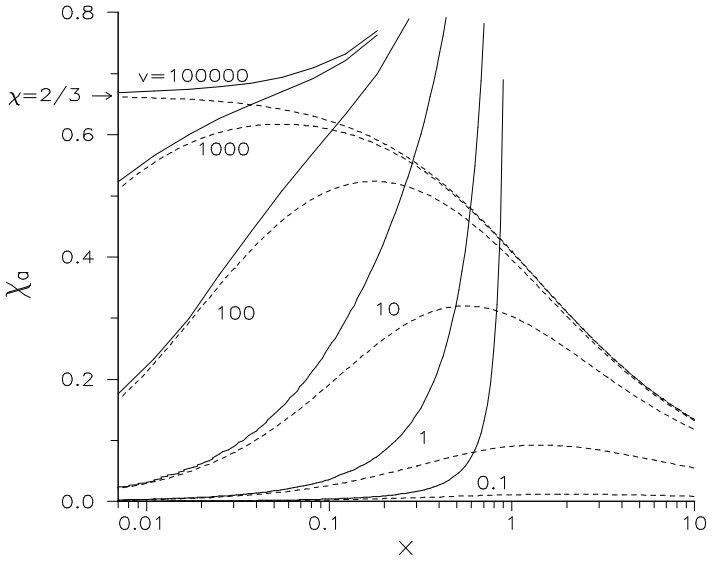

Figure 3. The effective critical exponent χ_a versus scaled distance from the seed surface $x = h/R$ for both concave (broken curves) and convex (full curves) geometries at different values of $V = aR\rho_0^{1/\chi}/(1-\chi)$. Arrow shows the classical value of $\chi = \frac{2}{3}$ for the planar geometry.

We can define from (1) the apparent value of the critical exponent χ_a as

$$\chi_a = -\frac{\mathrm{d}\ln N_{AB}}{\mathrm{d}\ln h}. \tag{17}$$

Figure 3 shows a plot of the apparent critical exponent χ_a versus scaled distance from the seed surface x for both concave (broken curves) and convex (full curves) geometries. We see that for propagation started from the curved seed line the value of the apparent exponent χ_a is not constant and strongly depends on x.

Not far from the seed surface, at $x \to 0$, with high initial density value $\rho_0 = \rho_{\max} \approx 1$ and the limit of $V \to \infty$, the intrinsic value $\chi_a = \chi = \frac{2}{3}$ is observed. The observed χ_a values substantially decrease with initial density decrease. The χ_a value always increases with the x increase for the IP case. For the OP case, the χ_a goes through the maximum. We should stress that these are only apparent changes of critical exponents, estimated on the basis of (17), because all calculations were done for the universal system in assumption of constancy of the intrinsic χ-value ($\chi = \frac{2}{3}$).

3.2. Numerical simulation

The dependencies of $y = \rho R^{\chi}$ upon $x = h/R$ obtained as results of numerical simulations are depicted in figure 4 for (*a*) the IP case and (*b*) the OP case. The different points correspond to different radii of the initial circular seed lines. All these data are for the case of the maximal initial density of domain boundary $\rho_0 = \rho_{\max} \approx 1$ with the ordered configuration of *A* and *B* species, as in the seed line (2). The continuum limit for this case corresponds to the situation where $R \gg 1$ and we can neglect the lattice discreteness. The full curves in figure 4 were obtained from (13) for the case of $\chi = \frac{2}{3}$, $V \to \infty$ in the continuum limit. We see that the coincidence between the results of the mean-field

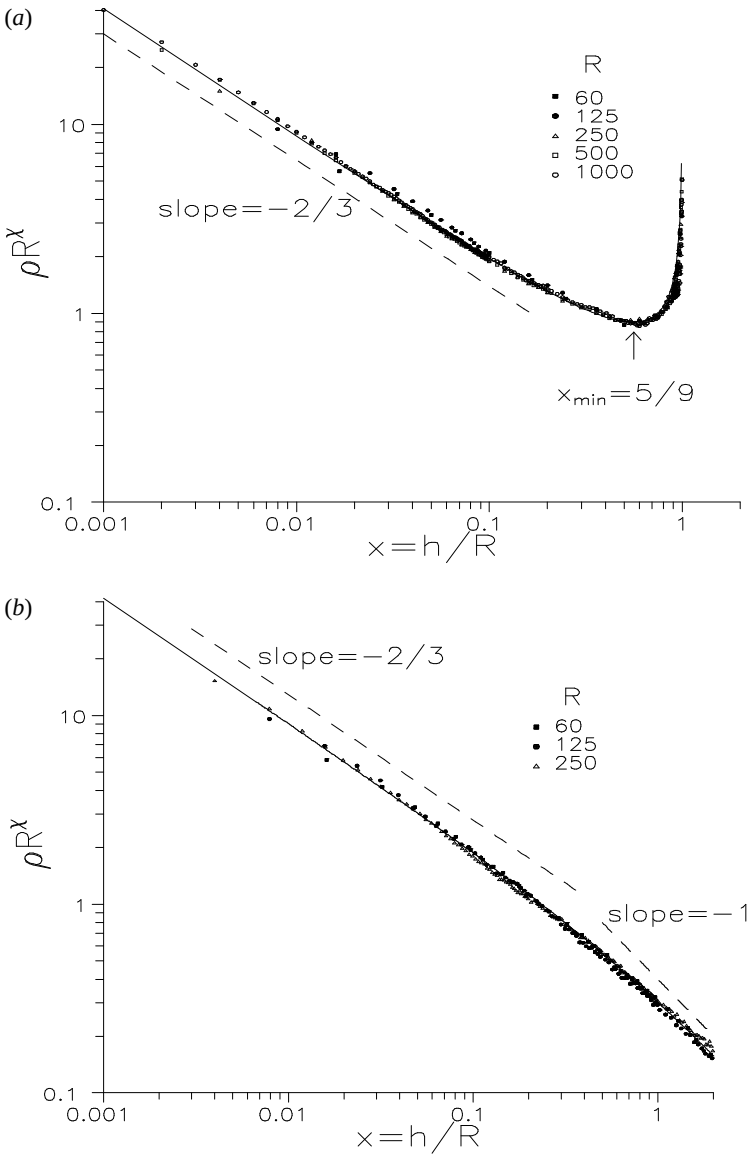

Figure 4. The scaled density $y = \rho R^{\chi}$ versus scaled height of the front $x = h/R$ for the growth spreading (a) inside the circular cavity and (b) outside the circular exclusion. The different points are the simulation results for different cavity (a) or exclusion (b) radii, as marked on the figures. All data are obtained for the limit case of $\rho_0 = \rho_{\max}$, for configuration shown by line (2). The full curves are obtained from the mean-field equation (13) where we used $a = 2.5 \pm 0.2$ (6) estimated by simulation for the case of planar geometry. Point of minimum $x = x_{\min} = \frac{5}{9} \approx 0.561$ is defined by the (15) for $\chi = \frac{2}{3}$.

approximation and the computer simulation is rather good. It is important to note that in the limit case of higher initial density of AB boundaries all data obtained at different values of R in the scaled coordinates ρR^{χ} versus $x = h/R$ fall on the same curves for both IP and OP cases.

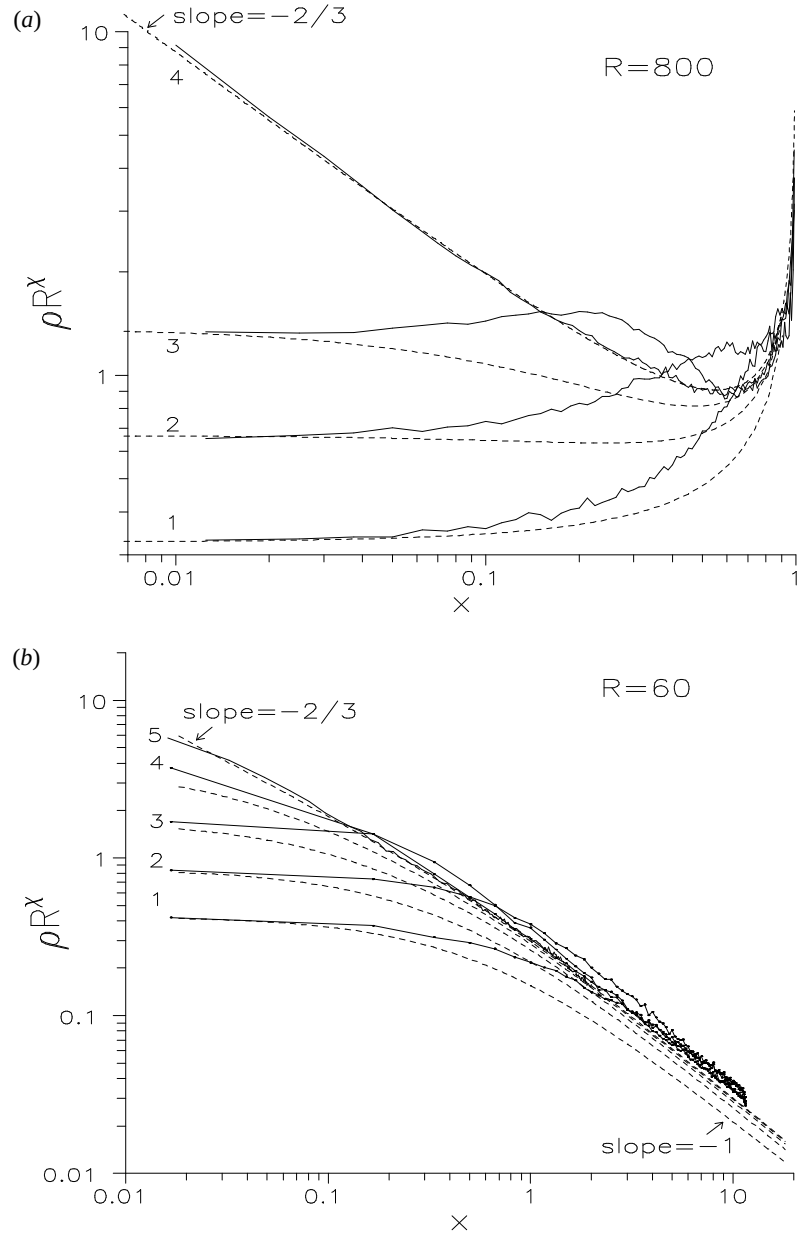

Figure 5. The scaled density $y = \rho R^{\chi}$ versus scaled height of the front $x = h/R$ for (*a*) the growth spreading inside the circular cavity or radius $R = 800$ and (*b*) outside the circular exclusion or radius $R = 60$. The full curves are the simulation results for different initial numbers of domain interfaces (*a*): $N^0_{AB} = 20(1), 40(2), 80(3), N_{\max}(4)$, and (*b*): $N^0_{AB} = 10(1), 20(2), 40(3), 90(4), N_{\max}(5)$. Broken curves are obtained for the same numbers of domain interfaces through the mean-field result (13) where we used $a = 2.5 \pm 0.2$ (6), estimated by simulation for the case of planar geometry.

For relatively small values of the initial density ρ_0, when we start propagation from a configuration with a limited number of domain boundaries, $N_{AB} \approx 10$–100, the simulation

results can deviate substantially from the predictions of mean-field theory, as is shown in figure 5 for (*a*) the IP case and (*b*) the OP case. The reason for such deviation is far from clear, but we think that it may simply reflect the limitations of the mean-field approach which follow from neglecting the long-range correlations between the AB domain boundaries.

4. Conclusions

We conclude that the apparent critical exponent χ_a determined on the basis of (17) through analysis of results of numerical experiments for the SMK model is not universal or of constant value. In the case of nonplanar geometry, the apparent critical exponent χ_a depends on the AB front height, the initial number of AB domains and on the type of growth geometry. This conclusion remains true for the SMK model even when the model preserves its internal universality defined by the classical critical exponent $\chi = \frac{2}{3}$. The best agreement between numerical simulation and mean-field approximation results is observed only at a high initial number of boundaries N^0_{AB}. At a low initial number of boundaries N^0_{AB}, the mean-field approximation allows only a qualitatively true description. In this case, the absence of quantitative description may be explained by the effect of long-range correlations, which result in faults in the mean-field description.

We believe, that the results obtained in this paper coincide qualitatively quite well with data presented in [10]. The authors there have shown that for an initial configuration consisting of only two species (AB) the number of boundaries is approximately conserved at the level of $N_{AB} \approx 2$ and for this case they have obtained $\chi_a \approx 0$. Assuming that for propagation under such conditions $N^0_{AB} = 2$, $R \approx 1$, $\chi = \frac{2}{3}$ and the value $a = 2.5 \pm 0.2$ (6), we get $V \approx 1$ as estimated from (12). As follows from our data presented in figure 3, when V is so low, the χ_a value is small and practically equal to zero at high-enough distances from the seed centre, which is in correlation with the data obtained in [10]. We believe that such apparent alterations of criticality or scaling exponential functions may occur in other models of radial growth, as was observed e.g. in [20] for the Eden model. Similar problems are worthy of further investigation with an extended range of models, system component numbers and space dimensionality etc.

Acknowledgments

We are grateful to Marcel Ausloos, Barbara Drossel, Miroslav Kotrla, Sujata Tarafdar, and Nicolas Vandewalle for providing us with preprints of their works and useful correspondence, and we thank Natalija Pivovarova for help with preparation of the manuscript. This work is partly supported by a grant QSU082112 from ISSEP.

References

[1] Feder J 1988 *Fractals* (New York: Plenum)
[2] Takayasu H 1990 *Fractals in the Physical Sciences* (Chichester: Wiley)
[3] Avnir D (ed) 1992 *The Fractal Approach to Heterogeneous Chemistry: Surfaces, Colloids, Polymers* (Chichester: Wiley)
[4] Viscek T 1992 *Fractal Growth Phenomena* (Singapore: World Scientific)
[5] Barabási A-L and Stanley H E 1995 *Fractal Concepts in Surface Growth* (Cambridge: Cambridge University Press)
[6] Meakin P 1998 *Fractals, Scaling and Growth Far From Equilibrium* (Cambridge: Cambridge University Press)
[7] Ren S Z, Tombácz E and Rice J A 1996 *Phys. Rev.* E **53** 2980

[8] Tarafdar S and Shashwati R 1998 *Physica* **B** to be published
[9] Saito Y and Muller-Krumbhaar H 1995 *Phys. Rev. Lett.* **74** 4325
[10] Vandewalle N and Ausloos M 1996 *Phys. Rev.* E **54** 3006
[11] Drossel B and Kardar M 1997 *Phys. Rev.* E **55** 5026
[12] Kotrla M and Predota M 1997 *Europhys. Lett.* **39** 251
[13] Kotrla M, Predota M and Slanina F 1998 *Surf. Sci.* to be published
[14] Batchelor M T, Henry B L and Watt S D 1998 *Physica* **A** to be published
[15] Vandewalle N and Ausloos M 1995 *Phys. Rev.* E **52** 3447
[16] Vandewalle N, Ausloos M and Cloots R 1996 *J. Cryst. Growth* **169** 79
[17] Eden M 1958 *Symposium on Information Theory in Biology* ed H P Yockey (New York: Pergamon) p 359
[18] Derrida B and Dickman R 1991 *J. Phys. A: Math. Gen.* **24** L191
[19] Lebovka N I, Vygornitskii N V and Mank V V 1997 *Colloid. J.* **59** 310
[20] Batchelor M T, Henry B L and Watt S D *Physica* **A** to be published
[21] Smoluchowsky M V 1917 *Z. Phys. Chem.* **92** 129
[22] Bramson M and Griffeath D 1980 *Ann. Prob.* **8** 183
[23] Torney D C and McConnell H M 1983 *J. Phys. Chem.* **87** 1941